Welding to Pipe Column under Axial Compressive Load†

Hiroyuki SUZUKI* and Kohsuke HORIKAWA**

Abstract

In the case of strengthening of existing structures by welding under loading, compressive members may buckle during welding because welding heat input decreases Young's modulus and yield strength. Even though buckling does not occur during strengthening works, load carrying capacity of the members may decrease less than that of members welded without loading, as welding under compressive load causes larger deformation and introduces additional residual stress in the members.

In this paper, pipes were welded under axial compressive loading to study the stability during welding. Next, load carrying capacity of those pipes which were stable during welding were examined.

KEY WORDS: (Strengthening Welding) (In-service Condition) (Buckling) (Load Carrying Capacity) (Pipe Column)

1. Introduction

There are two means in the dealing with decreasing of load carrying capacity of existing structures and/or increasing of applied load. One is the construction of new structure and the other is the repair and/or the strengthening of existing structure. The former is selected in the case of great decreasing of load carrying capacity and/or great increasing of applied load and the latter is selected in the other cases. The repair and/or strengthening works show a tendency to increase, recently[1].

Remove or reduction of load does not need in strengthening works if the works can be performed under loading. Moreover, drilling holes and covering up the loss of cross sectional area don't need if welding can be used in connection of members in strengthening works under loading. However, as there are few studies in relation to welding under loading, welding is not generally used yet. So, high-tension bolt connection is used in many cases.

It is necessary to examine the followings in the case of welding to members under loading.

1) Stability during welding – High temperature region spreads because of giving welding heat and has low Young's modulus and yield strength. Therefore, rigidity and load carrying capacity of structure decrease temporarily.
2) Load carrying capacity after works – Large deformation and additional residual stress are introduced by welding under loading in the member. So, load carrying capacity of the member may decrease.

The effect of welding under loading on members differs by the kind of applied load. Crack may occur in weld zone in tensile members and buckling may occur in compressive members[2].

In this paper, pipes were welded under axial compressive loading to study the stability during welding. Next, load carrying capacity of those pipes which were stable during welding were examined.

2. Experimental Procedure

2.1 Specimen

Specimens are carbon steel pipe of 410 MPa in the tensile strength (hereinafter called STK 41). There is the great difference between short column and long column when the mechanical behaviors of columns are considered. In this study, pipes of 216.3 mm in outer diameter x 5.8 mm in thickness x 1600 mm in length and 48.6 mm x 2.4 mm x 1600 mm were used as short and long column. Slenderness ratios ($\lambda = l/r$) are 21.5 and 97.7 in the case of considering effective buckling length (l) as 1600 mm.

Considering that attachments are welded to column under loading, there are two cases in this work; weld line is in parallel with applied load and transverse to applied load. In this experiment, gusset plate and ring stiffener are

† Received on October 31, 1984
* Research Associate
** Associate Professor

Transactions of JWRI is published by Welding Research Institute of Osaka University, Ibaraki, Osaka 567, Japan

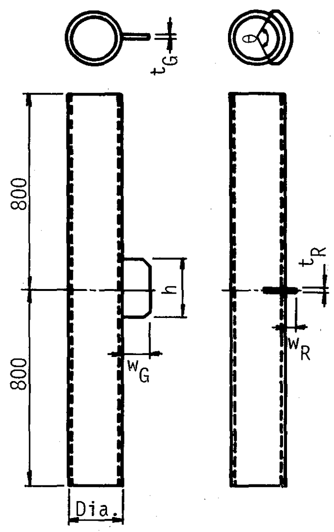

Dia.(mm)	t_G(mm)	h(mm)	w_G(mm)	t_R(mm)	w_R(mm)	θ(°)
216.3	9	200	100	9	50	120
48.6	9	150	50	9	30	120

Fig. 1 Gusset plate and ring stiffener configurations

welded to column as examples of both cases. Gusset plate and ring stiffener configurations are shown in Fig. 1.

Mechanical properties of pipes are shown in Table 1. These were obtained from tensile test using three coupon test specimens.

Table 1 Mechanical properties

Dia.(mm)	Y.S.(MPa)	T.S.(MPa)	El.(%)
216.3	390	470	31
48.6	410	480	23

Experimental conditions are shown in Table 2. Nominal stress σ_n = 160 MPa, divided applied load by cross sectional area, is fundamental allowable stress in "Design standards on structures for transmissions" and σ_n = 240 MPa is yield stress of STK 41 in JIS G 3444. When attachments were welded to long column under fundamental allowable stress, load was unable to be controlled during welding. Therefore, welding to long column was performed under σ_n = 80 MPa being a half of fundamental allowable stress and σ_n = 100 MPa that was buckling allowable stress considering slenderness ratio. Besides B and C type specimens, A type specimen of 508 mm in outer diameter was only used for measurement of temperature distribution during and after welding.

By the way, "Load is unable to be controlled" is defined as "unstable" hereinafter and load at this time is called load carrying capacity.

2.2 Welding under loading

Members of electric transmission tower are considered in this experiment. Main leg of tower is load controlled member and diagonal bracing, sway bracing and so on are displacement controlled members because electric transmission tower is high order of statically indeterminate structure. Members may buckle by thermal stress in welding under displacement-restraint. However, this is a matter under consideration.

Experiment was performed under load control. Experimental procedures are the followings.

1) Set of the prescribed load
2) Tack welding of gusset plate or ring stiffener
3) Welding of gusset plate or ring stiffener
4) Holding the load during 20 minutes after welding
5) Unload

In B type specimen, teflon sheet was put between specimen and crosshead for reduction of horizontal restraint by friction force. End surfaces of specimen were machined as both surfaces became parallel with each other. As jigs were not used at ends, both ends were under the condition of fixed support.

Experiment of C type specimen was performed under the condition of hinged support at both ends because of use of the end fittings.

Table 2 Experimental conditions

	σ_n=0MPa	σ_n=80MPa	σ_n=100MPa	σ_n=160MPa	σ_n=240MPa
Gusset pl.	B-1-0			B-1-A	B-1-Y
Ring stiff.	B-2-0			B-2-A	B-2-Y
Gusset pl.	C-1-0	C-1-H	C-1-S	C-1-A	
Ring stiff.	C-2-0	C-2-H	C-2-S	C-2-A	

Code of specimen number

B-1-0
→ Magnitude of nominal stress
→ 1; Gusset plate, 2; Ring stiffener
→ B; Dia.=216.3mm, C; Dia.=48.6mm

Strain gauges were attached at the center of 4 generating lines of specimen to check the load and measure the eccentricity. Name of weld lines is shown in Fig. 2. Fillet weld was performed by manaul welding. Welding position and leg are shown in Table 3. GL and RU were welded first and GR and RL were welded secondly in gusset plate and ring stiffener, respectively. Welding conditions are shown in Table 4.

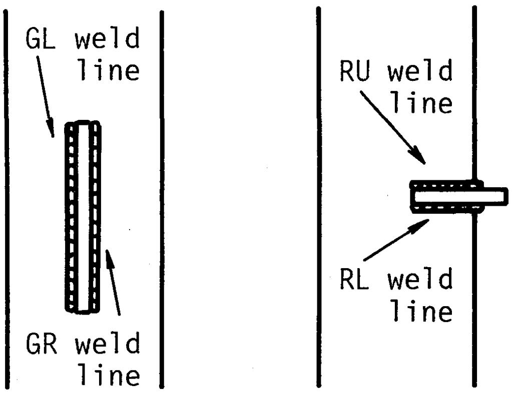

Fig. 2 Name of weld line

Table 3 Welding position and leg

	GL	GR
B-type	Vertical up 5mm	Vertical up 5mm
C-type	Vertical down 4mm	Vertical down 4mm
	RU	**RL**
B-type	Horizontal 5mm	Overhead 5mm
C-type	Horizontal 4mm	Overhead 4mm

Table 4 Welding conditions

Specimen	Current (A)	Voltage (V)	Weld speed (cm/min)	Heat input (kJ/cm)
B-1	135~140	23~25	7~9	21~29
B-2	155~180	25	10~14	17~24
C-1	150~160	25~27	30~43	6~8
C-2	120~130	22~25	12~19	9~14

Initial deformation was measured using thickness gauge before welding under loading. Locations of deformation measurement are shown in Fig. 3. Specimen has a seam because it is an electric welded pipe. Seam was put at line a in Fig. 3 in all specimen.

2.3 Load carrying capacity test

Load carrying capacity test was performed using the pipes which gusset plate or ring stiffener was welded in 2.2.

As B type specimen was loaded without end fittings, there was a probability of local buckling near end. Therefore, jigs called sleeve were inserted in the ends to prevent local buckling. Teflon sheet was put between sleeve and crosshead. This condition of end is equivalent to fixed support. So, slenderness ratio is 21.5/2 = 10.8.

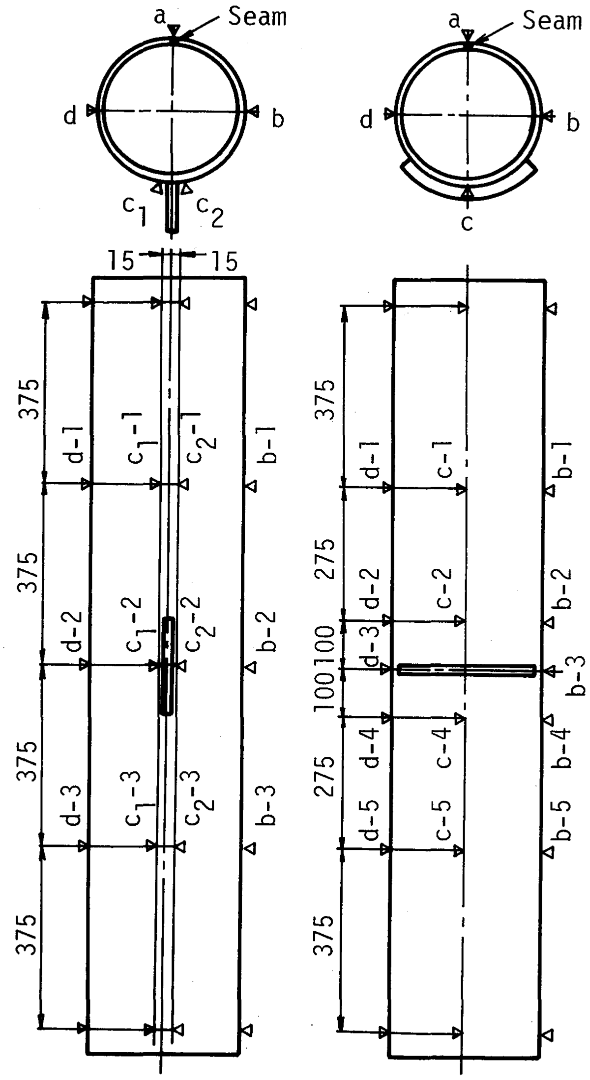

Fig. 3 Locations of deformation measurement

C type specimen was loaded using end fittings as mentioned in 2.2.

3. Results and discussions

3.1 Deformation behaviors during welding and conduction of weld heat

Even specimens applied σ_n = 240 MPa in B type specimen were stable during welding and till unloading. On the other hand, three of C type specimen became unstable during or after welding.

1) C-2-A . . . . during welding to RU
2) C-2-S . . . . during welding to RL
3) C-1-A . . . . after welding to GL and before welding to GR

Analytical consideration is performed to these specimens.

1) C-2-A specimen

C-2-A became unstable when RU was welded about 40 mm under compressive loading of σ_n = 160 MPa. Direction of deflection is shown in Fig. 4. Suppose that weld

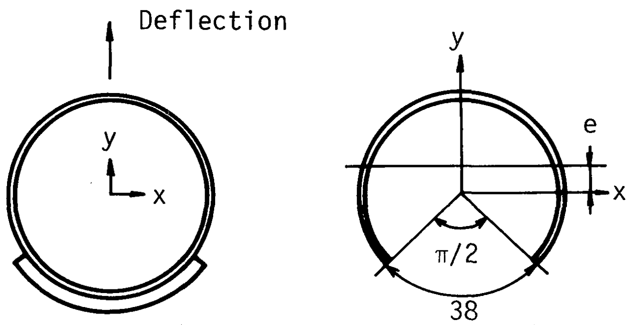

Fig. 4 Direction of deflection and analytical model of C-2-A and C-2-S specimens

length is 38 mm and rigidity of ring stiffener is negligible. Moreover, weld zone has not rigidity because it is melting or high temperature state. Therefore, weld zone is considered as the lack of cross sectional area. As a result of above assumptions, buckling load of the column having the section shown in Fig. 4 at the center can be found using secant formula. This buckling load is compared with applied load.

First, eccentiricity e is obtained by

$$e = \frac{G_X}{A} = \frac{2\sqrt{2}}{9\pi} \cdot \frac{D^2 + D \cdot d + d^2}{D + d}$$

where G_X is geometrical moment of area, A is area of cross section and D and d are outer and inner diameters. Eccentricity of this specimen becomes 7.0 mm. Buckling load can be found from secant formula using this eccentricity.

Secant formula is

$$\sigma = \frac{P}{A}\left(1 + \frac{e}{k'}\sec\frac{1}{2r}\sqrt{\frac{P}{EA}}\right) \qquad (1)$$

where P is external load, A is area of cross section, e is eccentricity, k′ is core radius, 1 is effective buckling length, r is radius of gyration of area and E is Young's modulus. Applying $|\sec\theta| \geqq 1$ to eq. (1) and considering that buckling occurs at $\sigma = \sigma_Y$,

$$P \leqq \frac{\sigma_Y \cdot A}{\frac{e}{k'} + 1} \qquad (2)$$

is derived from eq. (1). Namely, buckling occurs if applied load is not less than that of eq. (2).

Substituting the values in relation to C-2-A into eq. (2), $P \leqq 50$ kN is obtained. On the other hand, applied load was 56 kN. Consequently, it is considered that C-2-A became unstable. As a result of above discussion, safety during welding under compressive loading probably be estimated by treatment weld zone as the lack of cross sectional area.

2) C-2-S specimen

C-2-S became unstable during welding to RL under compressive loading of σ_n = 100 MPa. Weld length at that time was about 35 mm. Direction of deflection was the same as C-2-A (Refer to Fig. 4.). Eccentricity and buckling load are e = 7.0 mm and P_{cr} = 50 kN using the same model as C-2-A. Applied compressive load is 34 kN and corresponds to about 70% of buckling load. The reason of buckling under 50 kN is considered that yield stress and Young's modulus of the other part of weld zone reduced by conduction of welding heat of RU welded previous to RL.

Therefore, additional experiment was performed for the purpose of measurement of temperature distribution at unstable. This experiment was performed without loading. Welding conditions and locations of thermocouples are shown in Table. 5 and Fig. 5. Results are shown in Fig. 6. The time shown by dot-and-dashed line

Table 5 Welding conditions in the experiment of temperature distribution measurement

Specimen (Weld line)	Current (A)	Voltage (V)	Weld speed (cm/min)	Heat input (kJ/cm)
C-1 (GL)	135	25	31	6.5
(GR)	135	25	33	6.1
C-2 (RU)	140	25	23	9.1
(RL)	140	25	21	9.8

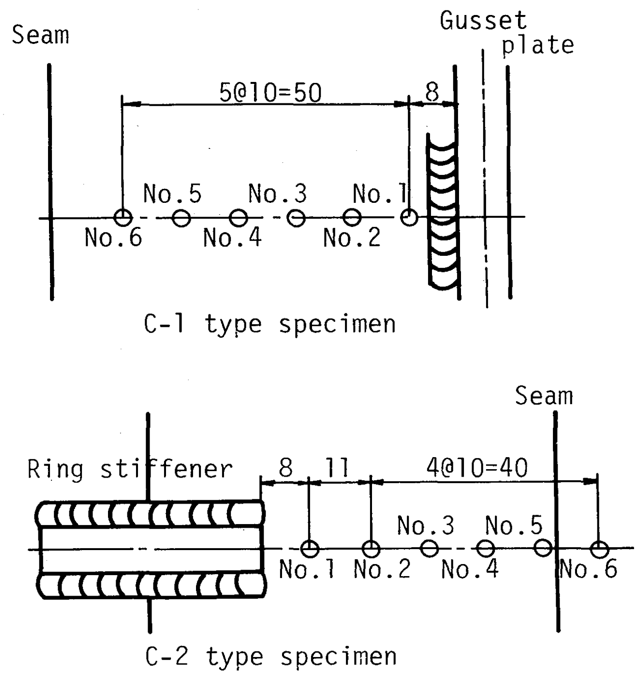

Fig. 5 Location of temperature measurement

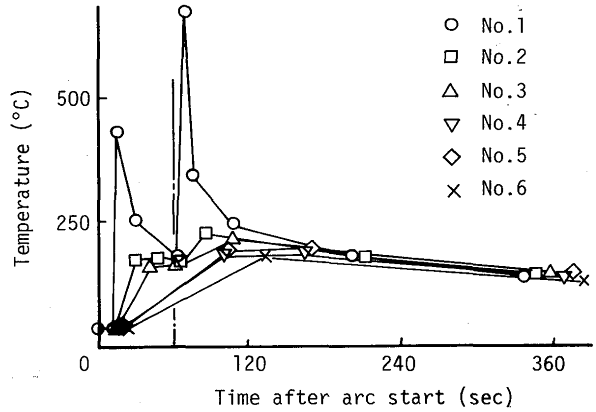

Fig. 6 Temperature of C-2 type specimen

is similar to one at unstable of C-2-S. Though No. 1 ~ 3 are about 170°C and No. 4 ~ 6 are about 100°C, temperature at the center section of specimen is assumed to be constant of 150°C for simplification of the following discussion.

Yield stress and Young's modulus at 150°C are shown to reduce to 75% and 85% of them at room temperature from tensile test in high temperature[3)].

As eq. (2) derived from secant formula doesn't include Young's moudlus, one of cross sectional area is substituted for reduction of Young's modulus using axial rigidity. Namely, the following equation is found from EA = const.

$$(0.85 \times E) \times A = E \times (0.85 \times A)$$

Consequently, eq. (2) becomes

$$P \leqq \frac{(0.75 \cdot \sigma_Y) \times (0.85 \cdot A)}{\frac{e}{k'} + 1} \quad \cdots\cdots\cdots\cdots (3).$$

Substituting the values in relation to C-2-S into eq. (3), $P \leqq 32$ kN is obtained. On the other hand, applied load was 34 kN. So, it is considered that C-2-S became unstable because eccentricity by the lack of cross sectional area and reduction of yield stress and Young's modulus by welding heat caused the reduction of load carrying capacity.

3) C-1-A specimen

C-1-A applied compressive loading of σ_n = 160 MPa became unstable after welding to GL. Direction of deflection is shown in Fig. 7.

Eccentricity is obtained by substituting the output of strain gauge after loading into secant formula.

$$e = 0.36 \text{ mm}$$

As this value is negligible small in comparison with outer diameter (D = 48.6 mm) being representative dimension,

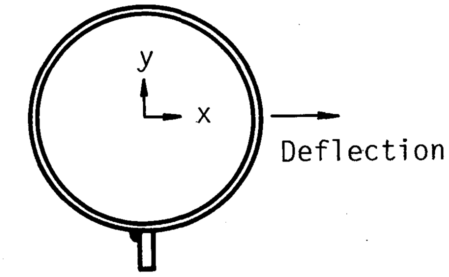

Fig. 7 Direction of deflection of C-1-A specimen

eccentricity can be neglected in this specimen.

Temperature measurement was performed because reductions of yield stress and Young's modulus were also considered in this specimen. Welding conditions and locations of thermocouples are shown in Table 5 and Fig. 5. Results are shown in Fig. 8. The time shown by dot-

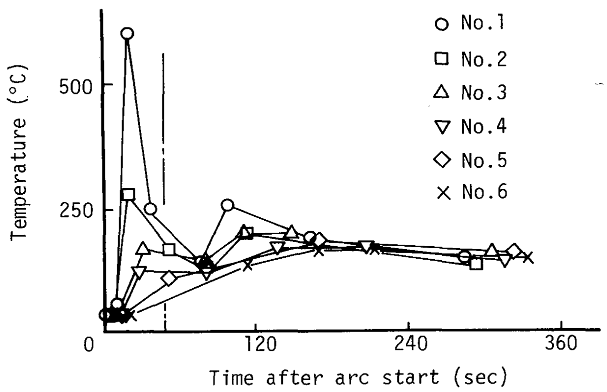

Fig. 8 Temperature of C-1 type specimen

and-dashed line is similar to one at unstable of C-1-A. Though the temperatures at this time are from 220°C to 70°C, temperature at this section is assumed to be constant of 150°C.

Buckling load can be obtained using Euler's formula because of neglect of eccentricity as mentioned above. $E' = 0.85 \cdot E$ is used in Euler's formula taking into account the effect of welding heat.

$$P_{cr} = \frac{\pi^2 E'I}{l^2} = 0.85 \times \frac{\pi^2 EI}{l^2} \quad \cdots\cdots\cdots\cdots (4).$$

Substituting the values of C-1-A into eq. (4), P_{cr} = 62 kN is obtained. Rigidity of gusset plate is neglected in this calculation. P_{cr} = 62 kN is 1.1 times as large as applied load P = 56 kN. The difference depends on neglect of eccentricity, assuming temperature distribution constant of 150°C, neglect of thermal strain by welding and so on.

It is considered that C-1-A became unstable due to reduction of Young's modulus by welding heat.

3.2 Load carrying capacity after welding

B-0-0 specimen which had no attachment was added in load carrying capacity test.

Deformations after welding of specimens which were stable during welding were measured using thickness gauge or vernier caliper. Results are shown in Table 6 with load carrying capacity. In this table, displacements of B-1 and C-1 type specimens are average of C_1-2 and C_2-2 in Fig. 3, and those of B-2 and C-2 type specimens are average of C-2 and C-4. Displacements before load carrying capacity test, called initial imperfection, are the sum of those before welding and by welding. Cave-in is plus. Examples of deformation after welding along line a in Fig. 3 are shown in Fig. 9.

Deformation increases obviously according to increase of applied load. C type specimen with small diameter shows larger deformation than B type specimen. When diameter is the same, pipe welded ring stiffener shows larger deformation than gusset plate. This reason is that weld length in cross section is long in the case of welding of ring stiffener.

The difference in maximum load is recognized between C-2-0 and C-2-H. This is considered to be the effect of initial imperfection. However, in the others, maximum load is nearly equal to each other in the same type specimen regardless of initial imperfection.

Table 6 Initial imperfection and maximum load

Specimen No.	Initial imperfection	Maximum load
B-0-0	<0.1 mm	1430 kN
B-1-0	0.5	1410
B-1-A	1.8	1400
B-1-Y	3.0	1450
B-2-0	1.4	1390
B-2-A	3.4	1370
B-2-Y	4.4	1420
C-1-0	1.7	57
C-1-H	2.9	56
C-1-S	3.8	58
C-2-0	2.1	60
C-2-H	6.1	50

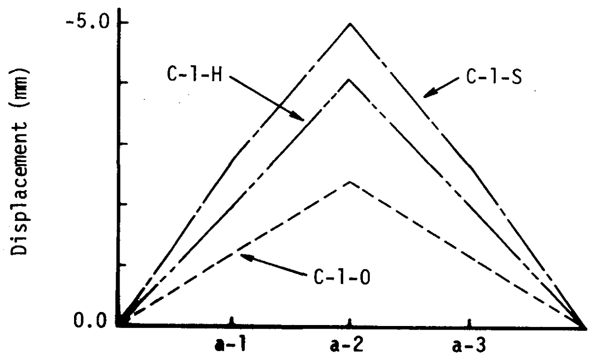

Fig. 9 Deformation of C-1 type specimen after welding

3.3.1 B type specimen

Load-displacement curves are shown in Fig. 10 and 11. There is very little difference in all the specimens. Rigidity changes at 1200 kN and maximum load is 1370 ~ 1450

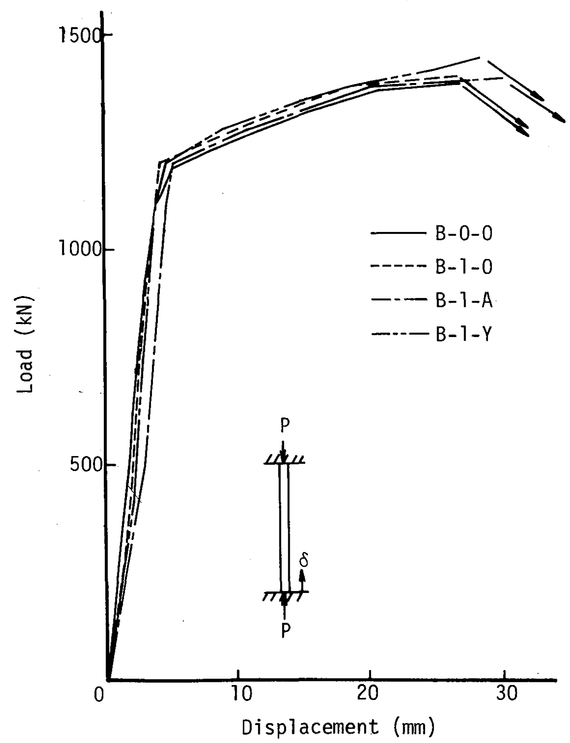

Fig. 10 Load-displacement curves of B-0-0, B-1-0, B-1-A and B-1-B-1-Y specimens

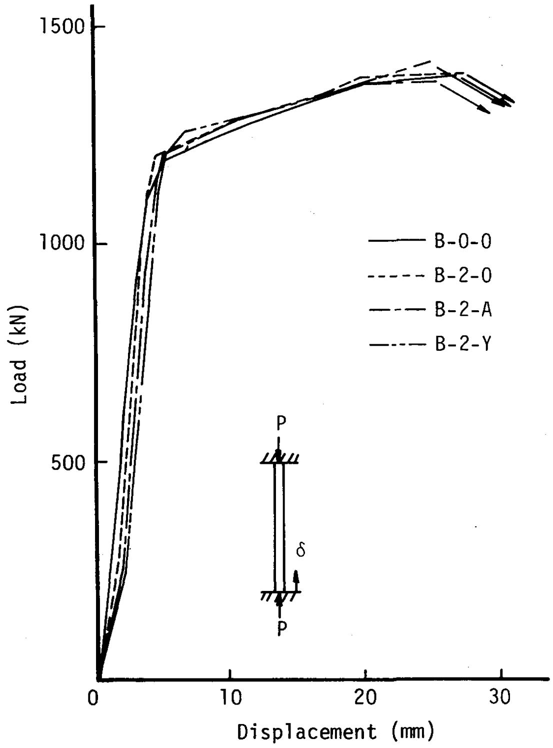

Fig. 11 Load displacement curves of B-0-0, B-2-0, B-2-A and B-2-B-2-Y specimens

$P_Y = \sigma_Y \cdot A = 390 \times 3800 = 1500$ kN

where σ_Y = 390 MPa is the result of tensile test using coupon test specimen machined from B type specimen. Even maximum load of B-0-0 having no attachment is under yield load. The reasons are considered to be the difference of tensile yield stress of base plate from compressive yield stress of pipe, the effect of residual stress introduced during manufacturing, Bauschinger effect and others. Though additional residual stress is introduced in the specimens welded with or without loading, their load-displacement curves are nearly equal to one of B-0-0. Consequently, even though gusset plate of 200 mm in length or ring stiffener of 230 mm in length is welded to pipe of 10.8 in slenderness ratio and 216.3 mm in outer diameter with compressive loading of $\sigma_n \leqq 240$ MPa and residual stress distribution changes locally as a result of welding, load carrying capacity of it is considered to be not less than not only one of pipe welded without loading but also one of pipe welded no attachment. Yield load is 910 kN using σ_Y = 240 MPa, yield stress of STK 41 in JIS G 3444. All load carrying capacity of specimen had the factors of 1.5 ~ 1.6 of this yield load.

3.3.2. C type specimen

Load-displacement curves of specimens which were stable during welding are shown in Fig. 12. Direction of deflection at unstable during loading is shown in Fig. 13.

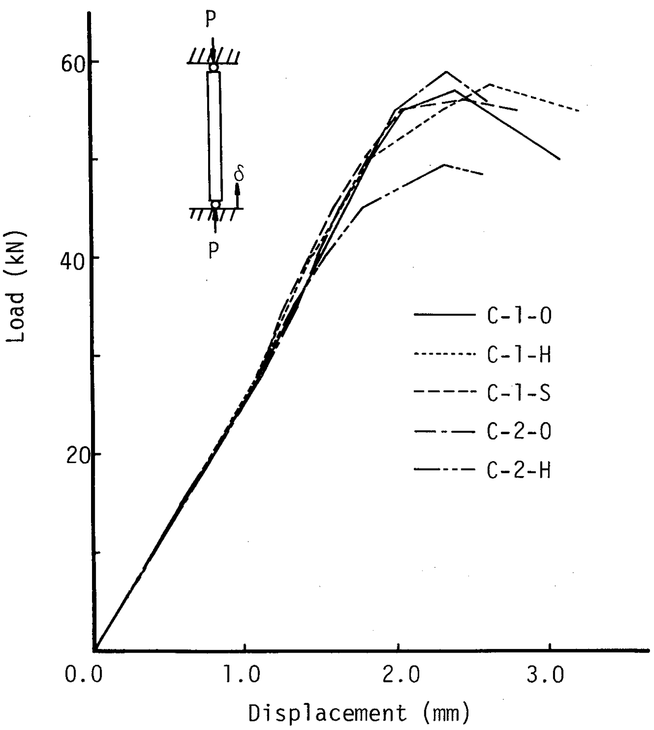

Fig. 12 Load-displacement curves of C-1 and C-2 type specimens

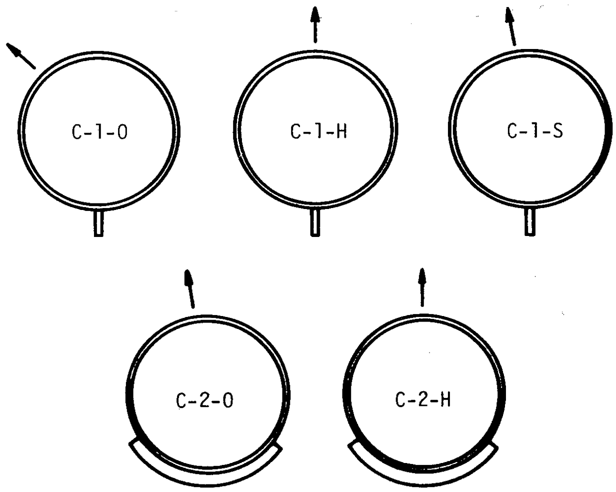

Fig. 13 Direction of deflection

Load carrying capacities of C-1 type specimen were 56 kN to 58 kN regardless of applied load during welding. There is no significant difference among them. Even C-1-0 welded without loading has not a little deformation as shown in Table 6 and Fig. 9 and C-1-H and C-1-S welded with loading have about two times as much deformation as C-1-0. It is considered that this deformation causes specimen to deflect to the direction shown in Fig. 13.

Let's find the buckling load of C-1 type. Displacement of a-2 shown in Fig. 9 is used for the representative value of deformation before loading though this doesn't all correspond to displacement of direction of deflection. Displacements of a-2 in all specimen were as follows.

C-1-0 . . . . 2.4 mm
C-1-H . . . . 4.1 mm
C-1-S . . . . 5.0 mm

Although these specimens are columns stiffened locally, the rigidity of gusset plate is neglected in the following calculation because the ratio of the length of gusset plate to pipe is about 0.1. Suppose that initial deflection curve is sine one. Provided initial deflection curve is expressed using

$$V_0 = \alpha \cdot \sin \frac{\pi x}{l} \quad \text{. . . . .} \quad (5),$$

additional deflection curve by loading becomes

$$V = \frac{P}{P_e} \times \frac{\alpha \cdot \sin(\pi x/l)}{1 - P/P_e} \quad \text{. . . . . .} \quad (6)$$

where $P_e = \pi^2 EI / l^2$. So, eccentricity at loading is obtained from eqs. (5) and (6).

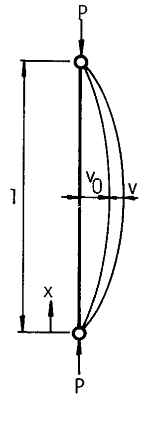

$$e = V_0 + V$$

$$= \frac{1}{1 - P / P_e} \times \alpha \times \sin \frac{\pi x}{l} \quad \ldots\ldots\ldots\ldots (7)$$

As bending moment at this time is

$$M = P \cdot e = \frac{P \cdot \alpha \cdot \sin (\pi x/l)}{1 - P / P_e} \quad \ldots\ldots\ldots\ldots (8),$$

maximum stress at the center section of sepcimen (x/l = 1/2) becomes

$$\sigma = \frac{P}{A} + \frac{M}{W} = \frac{P}{A} \left(1 + \frac{e}{k'} \right) \quad \ldots\ldots\ldots\ldots (9).$$

Assuming that buckling occurs at $\sigma = \sigma_Y$, eq. (9) coincides with eq. (3) derived from secant formula.

Substituting eccentricity at the center section of specimen (x/l = 1/2) given by eq. (7) into eq. (9), buckling load can be found.

Let's obtain buckling load of C-1-0 as an example. First, substituting $I = 8.99 \times 10^4$ mm^4, l = 1600 mm, E = 2.1×10^5 MPa, α = 2.4 mm and x/l = 1/2 into eq. (7), eccentricity at the center of specimen is given as shown by dashed line in Fig. 14. Next, substituting this eccentricity, σ_Y = 410 MPa, A = 335 mm^2 and k' = 11.1 mm into eq. (9), buckling load is obtained as shown by solid line in Fig. 14. Load of intersection of dashed and solid lines is buckling load in this analysis. It is a good agreement to maximum load (dot-and-dashed line) in experiment. The reasons why experimental value shows a little lower than analytical value may be that initial displacement used in this analysis did not correspond to it in the direction of deflection in experiment, initial deflection curve was assumed to be sine one and others. Table 7 shows maximum load and buckling load obtained by the same way. No significant difference is recognized among buckling loads of C-1-0, C-1-H, and C-1-S. Therefore, load carrying capacity of pipe with slenderness ratio of 97.7, which is welded gusset plate of 150 mm in length with compressive loading of $\sigma_n \leqq 100$ MPa, is considered to be nearly equal to it of pipe welded without loading.

There was a difference of about 10 kN in maximum load between C-2-0 and C-2-H, as shown in Fig. 12. Direction of deflection is shown in Fig. 13. Using displacement of a-3 (see Fig. 3) for the representative value of deformation before loading, they were as follows.

Table 7 Comparison between maximum load in experiment and buckling load

Specimen No.	Maximum load	Buckling load
C-1-0	57 kN	60 kN
C-1-H	56	54
C-1-S	58	52
C-2-0	60	61
C-2-H	50	48

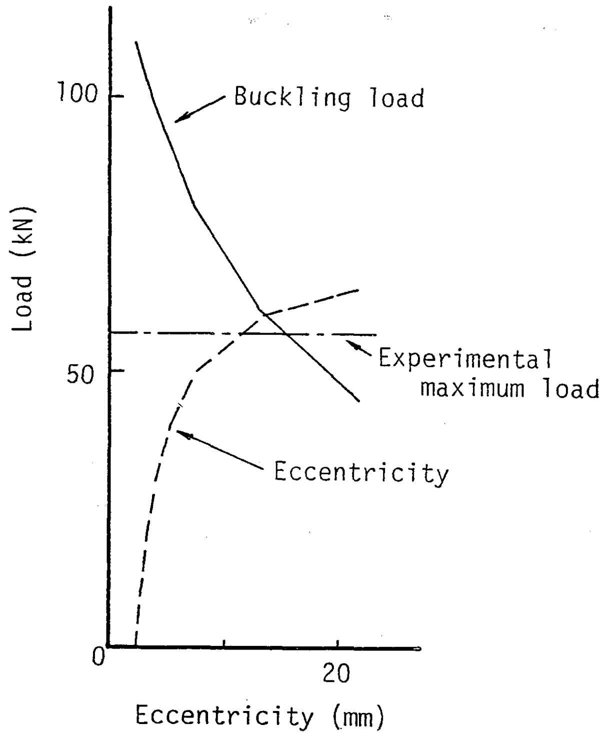

Fig. 14 Comparison between experimental maximum load and buckling load of C-1-0 specimen

C-2-0 .... 2.2 mm
C-2-H .... 7.0 mm

The difference between these displacements may cause the difference between both maximum loads.

Finding the buckling loads of C-2-0 and C-2-H by the same way as above mentioned, they become 61 kN and 48 kN. These are good agreements to maximum loads in experiment, respectively, as shown in Table 7. There is also a difference of 13 kN in buckling load. This is the effect of initial deflection, that is, welding under compressive loading.

Load carrying capacity of pipe with slenderness ratio of 97.7, which is welded ring stiffener of 50 mm in length with compressive loading of σ_n = 80 MPa is considered to reduce to 80% of it of pipe welded without loading.

4. Conclusions

Pipes with slenderness ratios of 10.8 and 97.7 were welded under compressive loading in order to attach gusset plate or ring stiffener. First, the stability during works was studied. Secondly, load carrying capacity of those pipes which were stable during works were examined. Pipes with slenderness ratio of 10.8 and 97.7

were columns showing inelastic and elastic buckling. Conclusions are as follows.

I) Stability during works

1) In pipe with slenderness ratio of 10.8, gusset plate of 200 mm in length or ring stiffener of 230 mm in length could be welded even under compressive loading of σ_n = 240 MPa being yield stress of STK 41 in JIS G 3444.

2) In the case of welding gusset plate of 150 mm in length to pipe with slenderness ratio of 97.7, pipe was stable under compressive loading of $\sigma_n \leqq 100$ MPa but became unstable during welding under compressive loading of σ_n = 160 MPa being fundamental allowable stress in JEC-127.

In the case of welding ring stiffener of 50 mm in length, pipe was stable under $\sigma_n \leqq 80$ MPa but became unstable during welding under $\sigma_n \geqq 100$ MPa. Therefore, some means which reduce applied load, lower welding heat input, divide weld length into some parts and so on, need for the purpose of prevent the unstable.

3) Analysis was performed for specimens which became unstable during welding. In this analysis, treating weld zone as lack of cross section and/or reduction of Young's modulus and yield stress by welding heat were considered. Consequently, this analysis was appropriate as the first approximation.

II) Load carrying capacity after works

4) Though pipes with slenderness ratio of 10.8, which were welded the attachment, had initial deflection of 4.4 mm in maximum, load carrying capacities of them had no significant difference and were nearly equal to pipe welded nothing. Therefore, load carrying capacity of pipe with slenderness ratio under 10.8, which is welded gusset plate under 200 mm in length or ring stiffener under 230 mm in length with compressive loading of $\sigma_n \leqq 240$ MPa, is considered to become not less than not only that of pipe welded without loading but also that of pipe welded nothing.

5) Load carrying capacities of pipes with slenderness ratio of 97.7, which were welded gusset plate of 150 mm in length with compressive loading of $\sigma_n \leqq 100$ MPa, had no significant difference and were nearly equal to that of pipe welded without loading. Load carrying capacity of pipe with slenderness ratio of 97.7, which was welded ring stiffener of 50 mm in length with compressive loading of σ_n = 80 MPa, reduced to about 80% of that of pipe welded without loading. Consequently, some means which reduce applied load, correct under compressive loading the deformation by welding and so on, need in this case.

Acknowledgement

The authors wish to thank to Mr. Y. Nakatsuji, Research Assistant, Welding Research Institute of Osaka University, and to Mr. S. Yamanaka and others, Japan Bridge Co., Ltd., for their cooperation in experiment.

References

1) Repair and strengthening, The bridge and foundation engineering, Vol. 17, No. 8, 1983 (in Japanese).

2) H. Suzuki and K. Horikawa: Deformation behaviors of plates welded under loading, Proc. of JSCE, No. 350/I-2, 1984-10 (in Japanese).

3) Tensile test of SS 41 in high temperature, private report (in Japanese).

4) The Japanese Electrotechnical Committe: Design standards of structures for transmissions, JEC-127-1979 (in Japanese).

5) Society of steel construction of Japan: Mechanical properties of plastically worked steels – On mechanical properties in tension and compression of STK 41–, JSSC, Vol. 6, No. 53, 1970, P.P. 1 ~ 34 (in Japanese).

6) Society of steel construction of Japan: Residual stress and buckling, JSSC Vol. 3, No. 16, 1967, P.P. 16 ~ 22 and P.P. 44 ~ 48 (in Japanese).

7) K. Horikawa, H. Suzuki and K. Imi: Repair welding on bridges in service condition, Trans. of JWRI, Vol. 12, No. 2, 1983, P.P. 149 ~ 155.

8) H. Suzuki and K. Horikawa: Fundamental study on welding to bridge members in service condition – Welding to compression members–, Trans. of JWRI, Vol. 12, No. 2, 1983, P.P. 143 ~ 147.